Yamano et al. Earth, Planets and Space 2014, 66:126
http://www.earth-planets-space.com/content/66/1/126

Earth, Planets and Space
a SpringerOpen Journal

LETTER Open Access

Heat flow survey in the vicinity of the branches of the megasplay fault in the Nankai accretionary prism

Makoto Yamano[1*], Yoshifumi Kawada[1] and Hideki Hamamoto[2]

Abstract

Heat flow measurements were conducted at four sites in the Nankai accretionary prism southeast of the Kii Peninsula, around the area where the megasplay fault reaches the surface, in conjunction with long-term monitoring of bottom water temperature at nearby stations. Analysis of the obtained data showed that variations in bottom water temperature seriously affect surface heat flow measurements in the areas with water depths of less than about 2,800 m. This effect can reach up to 20% to 30% and may have significantly contributed to a large scatter in the heat flow values previously measured in the study area. The temperature records were also used to determine heat flows from sediment temperature profiles disturbed by bottom water temperature variations. Results of measurements at sites deeper than 2,800 m indicate that the regional heat flow, corrected for surface disturbances including the influence of bathymetric relief, is about 65 mW/m^2, which is consistent with the value calculated using subduction thermal models. Local high heat flow values were obtained in the vicinity of the tips of the branches of the splay fault, suggesting advective heat transport by upward pore fluid flow along the faults.

Keywords: Nankai Trough; Heat flow; Accretionary prism; Splay fault; Cold seep; Bottom water temperature; Pore fluid

Findings

Introduction

Heat flow distribution around the trench is essential information for investigating the thermal structure of a subduction zone. Heat flow measured seaward of the trench reflects the temperature structure of the incoming oceanic plate, an important boundary condition for subduction thermal models. On the landward side of the trench, surface heat flow constrains the uncertain factors in thermal models, including frictional heating along the plate interface and radiogenic heat production in the overriding plate. However, the heat flow measured at the seafloor is often significantly disturbed by various processes near the surface, such as sedimentation, erosion, pore fluid flow, and bottom water temperature variation (e.g., Davis 1988). The observed heat flow may therefore not provide direct information on the temperature structure of the deeper part of the subduction zone.

In the Nankai subduction zone, where the Philippine Sea plate is subducting beneath southwest Japan, extensive heat flow measurements have been made around the Nankai Trough, mainly on the floor of the trough (around the trench axis) and in the accretionary prism that has developed landward of the trough (e.g., Kinoshita and Yamano 1995). The most concentrated measurements were made in the two target areas of deep-sea scientific drilling (the Ocean Drilling Program (ODP) and the Integrated Ocean Drilling Program (IODP)), the area off Muroto, southeast of eastern Shikoku, and the area off Kumano, southeast of the Kii Peninsula (Yamano et al. 2003; Hamamoto et al. 2011).

In the area off Kumano, Hamamoto et al. (2011) revealed the heat flow distribution on the landward side of the Nankai Trough, especially along the transect for IODP seismogenic zone drilling (NanTroSEIZE) (Tobin and Kinoshita 2006). This was accomplished by combining the values measured using ordinary surface probes and long-term monitoring instruments with those estimated from gas hydrate bottom simulating reflector (BSR) depths (Figure 1). Additional data were provided

* Correspondence: yamano@eri.u-tokyo.ac.jp
[1]Earthquake Research Institute, University of Tokyo, 1-1-1 Yayoi, Bunkyo-ku Tokyo 113-0032, Japan
Full list of author information is available at the end of the article

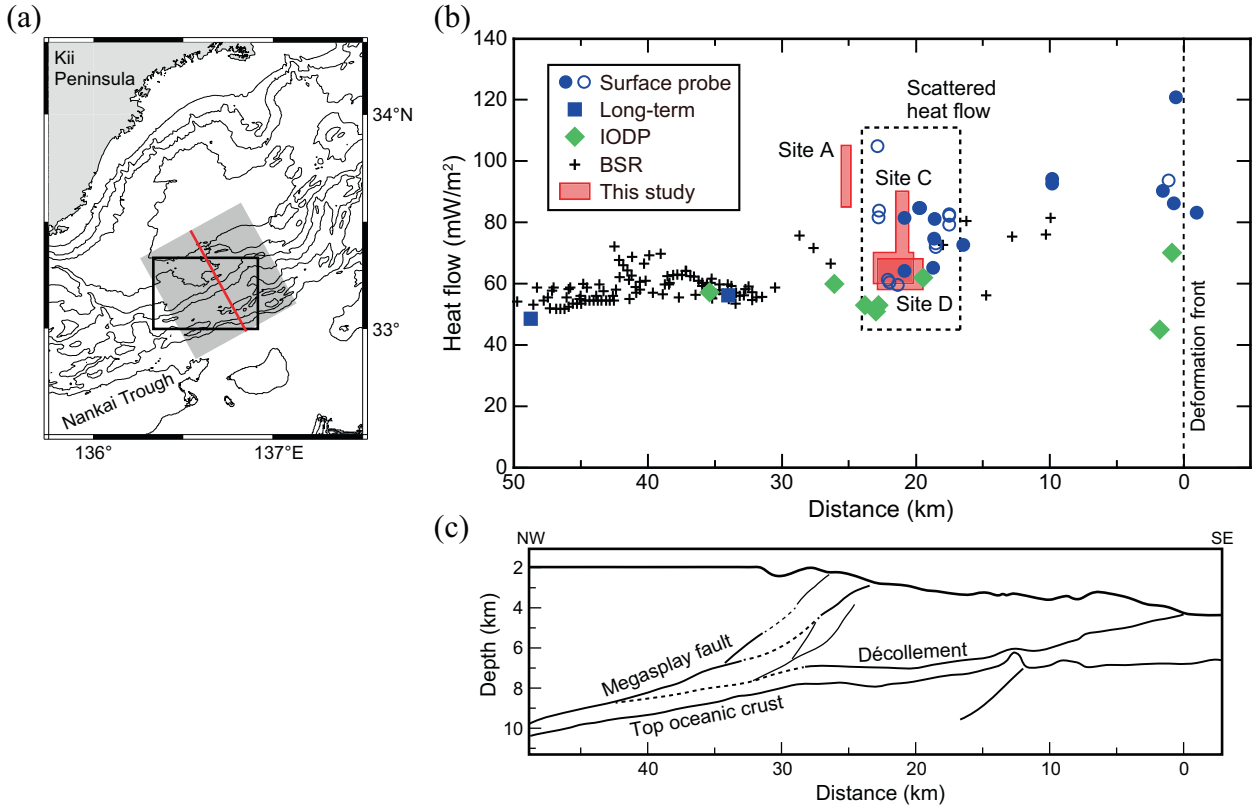

Figure 1 Heat flow data in the area southeast of the Kii Peninsula (off Kumano). (a) Location map. Heat flow data in the shaded area are plotted in the cross section in **(b)**. The solid line rectangle represents the study area shown in Figure 2. **(b)** Heat flow cross section along the red line in **(a)**. The horizontal axis is the distance from the deformation front (positive landward). Circles and squares are previous measurements with ordinary surface probes and long-term monitoring instruments, respectively (open circles: data of low quality) (Hamamoto et al. 2011; Kinoshita et al. 2008). Rhombuses are data obtained in IODP holes (Harris et al. 2013). Crosses are estimates from BSR depths (Ashi et al. 1999). Red shading indicates approximate ranges of values obtained in this study after correction for topographic effect. The dashed line rectangle indicates the high scatter zone. **(c)** Simplified bathymetry and structure cross section showing location of megasplay fault (modified from Moore et al. 2009).

by measurements in IODP drill holes (Harris et al. 2011, 2013). The large-scale heat flow distribution along the NanTroSEIZE transect was used to constrain thermal models of subduction in the off-Kumano area (Hamamoto et al. 2011; Harris et al. 2011; Spinelli and Harris 2011; Marcaillou et al. 2012), which estimated the temperature distribution and amount of frictional heating along the plate interface and heat transport by fluid circulation in the oceanic crust.

It should be noted that highly scattered heat flow values (60 to 100 mW/m^2) were obtained from the middle part of the accretionary prism slope, around 15 to 25 km landward of the deformation front (Figure 1). The large scatter implies that heat flow data in this anomalous zone (hereafter termed 'the high scatter zone') must be affected by some factor(s) within a few kilometers of the surface and cannot reflect the thermal structure in deeper parts of the subduction zone (e.g., plate interface). This inference is supported by the average of the scattered values, significantly higher than the surface heat flow calculated using the large-scale thermal models. On the other hand, detailed heat flow distributions in the high scatter zone may contain information on local tectonic processes. Since the high scatter was observed in the area where the megasplay fault system (Park et al. 2002; Park and Kodaira 2012) approaches and intersects the surface, it is possible that pore fluid flow along fault zones or mass movement associated with fault activity results in local heat flow variations. To extract such information from the observed heat flow data, we need to remove the influence of other disturbances.

In this study, we examined the influence of bottom water temperature variations quantitatively through long-term temperature monitoring. We also conducted concentrated heat flow measurements in the high scatter zone to estimate the heat flow from depths not disturbed by surface processes.

Possible causes of scattered heat flow

Taking account of the tectonic setting of the study area, the middle part of the accretionary prism slope in the

vicinity of the megasplay fault tip, we infer that the observed local variability of surface heat flow may be attributed to the following factors: seafloor topography, bottom water temperature variation, pore fluid flow along faults, and surface deformation.

Since the seafloor acts as a nearly isothermal boundary, the temperature field at a shallow depth is distorted below a rough topography. Surface heat flow increases in depressions and decreases over ridges. Harris et al. (2011) made corrections for the topographic effect on the heat flow values obtained at IODP holes and showed that the correction could be as high as +16% at Site C0006 (Figure 2). They applied the topographic correction to the existing surface probe data as well and found the effect to be small for data in the high scatter zone. Topographic disturbance is not negligible for measurements around fault scarps and is discussed in the 'Heat flow measurements in the high scatter zone' section.

Temporal variation in the bottom water temperature (BWT) causes a transient effect on the temperature distribution in sediments, resulting in disturbance of heat flow measurements with surface probes. In the off-Kumano area, nonlinear temperature profiles were often measured at stations with water depths of less than 2,100 m, indicating BWT variations with significant amplitudes (Hamamoto et al. 2005). To determine the heat flow by correcting for the influence of BWT variation, long-term monitoring of BWT was conducted at many stations in the off-Kumano area (Hamamoto et al. 2005, 2011), and BWT variation at a station at 2,525 m was found to be large enough to seriously disturb surface probe heat flow measurements. Harris et al. (2011) studied the relation between the existing surface probe data and the timing of the measurements and suggested that the scattered heat flow may be partly due to BWT variations at water depths down to approximately 3 km. We examine the influence of BWT variations in the 'Monitoring of bottom water temperature variation' section using new long-term temperature records in the high scatter zone.

Active faults cutting through accretionary prisms may act as permeable paths for pore fluid flow. Such localized fluid flow transports heat advectively and can raise heat flow around the location where the fault reaches the surface. Heat flow and/or temperature anomalies owing to upward fluid flow along faults were reported in some accretionary prisms, such as Cascadia and Barbados (e.g., Zwart et al.

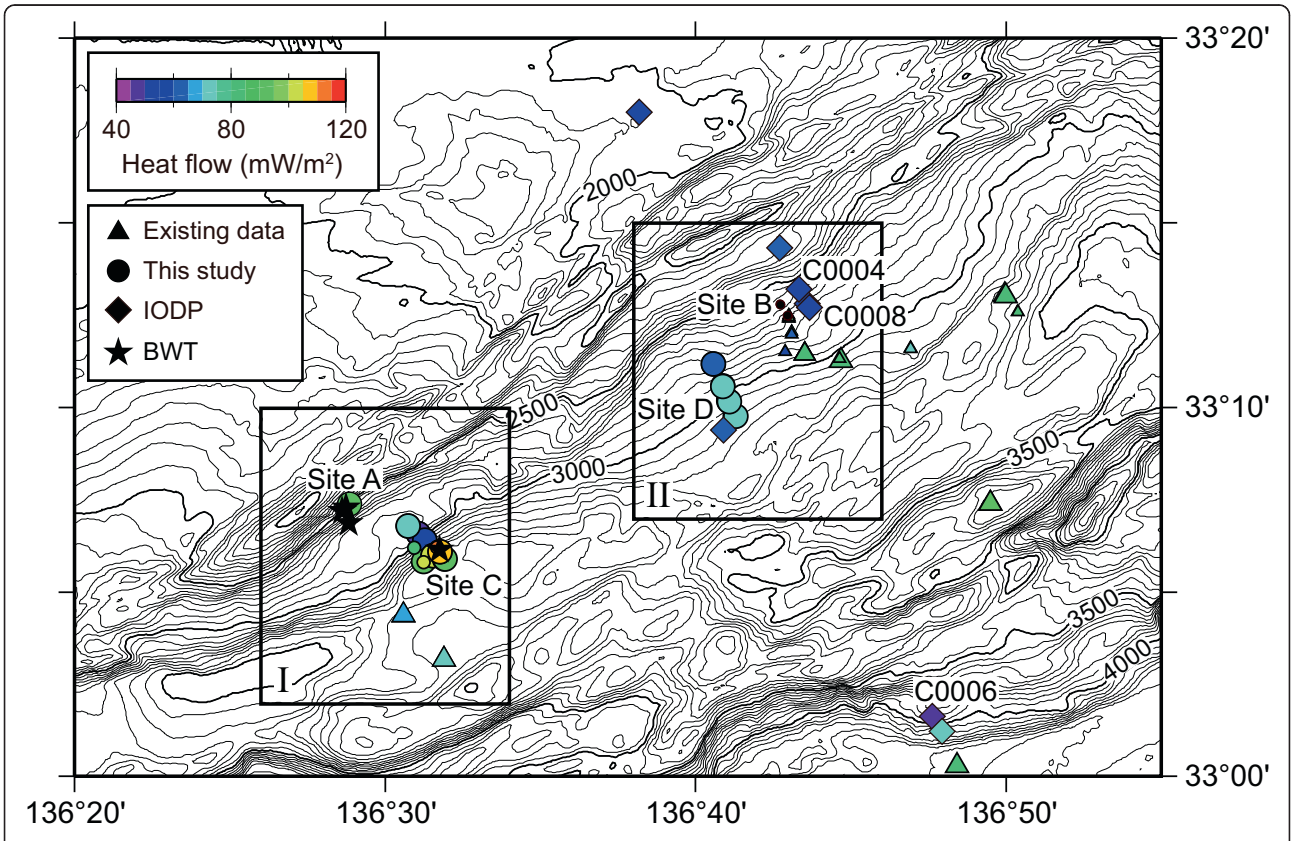

Figure 2 Heat flow data in the study area, color-coded by heat flow value. Triangles represent previous probe measurements. Circles represent this study. Rhombuses represent IODP holes. Smaller symbols are data of low quality. Stars indicate stations where bottom water temperature (BWT) monitoring was conducted.

1996; Foucher et al. 1990). In the Nankai Trough, local high heat flow anomalies accompanying thrust faults were detected at the toe of the prism in the eastern part of the trough (off Tokai) and in the off-Muroto area (Henry et al. 1992; Kawada et al. 2014). In the off-Kumano area, surveys with submersibles obtained high heat flow values at cold seep sites distributed along a branch of the megasplay fault (Goto et al. 2008). We attempted to detect similar heat flow anomalies through measurements with ordinary probes.

Sedimentation and erosion at the surface result in decrease and increase of surface heat flow, respectively. In the Nankai accretionary prism, which is tectonically active, various types of surface deformation may have caused movement of sediments, leading to disturbances in heat flow. Martin et al. (2004) showed that anomalies in BSR-derived heat flow in the prism slope off Tokai can be attributed to erosion and sedimentation due to slumping. In the off-Kumano area, Kinoshita et al. (2011) inferred that BSR depth variations in the frontal part of the prism reflect uplift and erosion caused by thrust faulting. In and around the high scatter zone, slump scars of submarine landslides are widely distributed (Kimura et al. 2011; Strasser et al. 2011) and may include very recent slumping events which can affect the surface heat flow.

Monitoring of bottom water temperature variation

To evaluate the effect of BWT variation on temperature distribution in surface sediments and correct for the effect, we conducted long-term monitoring of BWT at three stations with water depths of 2,530 m (WT1a), 2,555 m (WT1b), and 3,340 m (WT2) (Table 1; stars in Figures 2 and 3). Temperature measurements were made with a resolution of 1 mK for 28 months (March 2010 to June 2012) at WT1a and for 15 months (August 2010 to November 2011) at WT1b and WT2. WT1b is only about 250 m away from WT1a and shows essentially the same BWT variation as that of WT1a. BWT monitoring in the off-Kumano area was carried out for seafloor geodetic measurements as well by Osada et al. (2010). One of their stations (WT3) is located at an intermediate water depth, 2,755 m, between WT1a, WT1b, and WT2 (Table 1; Figure 3). The temperature records obtained at these stations (Figure 4) revealed the characteristics of BWT variations in the study area.

BWT variations at WT1a, WT1b, and WT3 have large amplitudes, about 0.15 K, comparable to those measured at water depths of 2,000 to 2,100 m (Hamamoto et al. 2011), whereas the variations at WT2 have much smaller amplitudes, less than 0.05 K. Spectral analysis shows that the variations at all the stations contain strong components with periods of around 40 to 60 days. All the records also exhibit very rapid variations, with a time scale of 1 h. These features are common to BWT records obtained in the off-Kumano area. It seems that a similar pattern of temperature variations occur in a wide range of water depths, but the amplitude decreases sharply somewhere between 2,755 and 3,340 m.

Using these temperature records, we calculated the influence of BWT variations on subsurface temperature distributions at WT1a, WT2, and WT3. The undisturbed temperature gradient, corresponding to heat flow from the deeper part and the thermal diffusivity of sediments were assumed to be 60 mK/m and 3.0×10^{-7} m^2/s, respectively, which are the typical values for the study area (Hamamoto et al. 2011). The calculated temperature profiles (Figure 5) demonstrate that temperature distributions in the upper 2 m are highly disturbed at WT1a and WT3. This should significantly affect heat flow measurements with short surface probes. At WT2, the influence of the BWT variation is much smaller, though it may not be negligible.

It is necessary to evaluate the effect of BWT variation more quantitatively in order to examine its possible contribution to the scattered heat flow. We constructed synthetic probe measurement data from the calculated disturbed profiles at various times: temperatures from four sensors at 0.3, 0.9, 1.5, and 2.1 m below the seafloor, supposing a partially penetrated probe, which is typical of the scattered heat flow data. Distinctly nonlinear temperature profiles were discarded, since temperature profiles in the scattered data set were apparently linear. We then determined the temperature gradient from the four temperature points using least squares fitting. The obtained gradient values range from 49 to 74 mK/m for WT1a and from 46 to 79 mK/m for WT3, compared to the undisturbed gradient of 60 mK/m. Variation in temperature gradient at WT2 is smaller, 54 to 66 mK/m for most of the observation period. The results imply that the effect of BWT variation may amount to 20% to 30% in the area shallower than about 2,800 m. At around 3,300 m, the

Table 1 Monitoring of bottom water temperature

Station	Coordinates	W. D. (m)	Observation period	Duration (days)	Amp. (K)
WT1a	33°07.32′N, 136°28.74′E	2,530	15 March 2010 to 11 July 2012	849	0.392
WT1b	33°07.22′N, 136°28.61′E	2,555	8 August 2010 to 7 November 2011	456	0.360
WT2	33°06.17′N, 136°31.75′E	3,340	14 August 2010 to 8 November 2011	451	0.108
WT3	33°06.91′N, 136°28.82′E	2,755	5 September 2008 to 4 December 2009	455	0.396

W. D., water depth; *Amp.*, peak-to-peak amplitude of observed temperature variation.

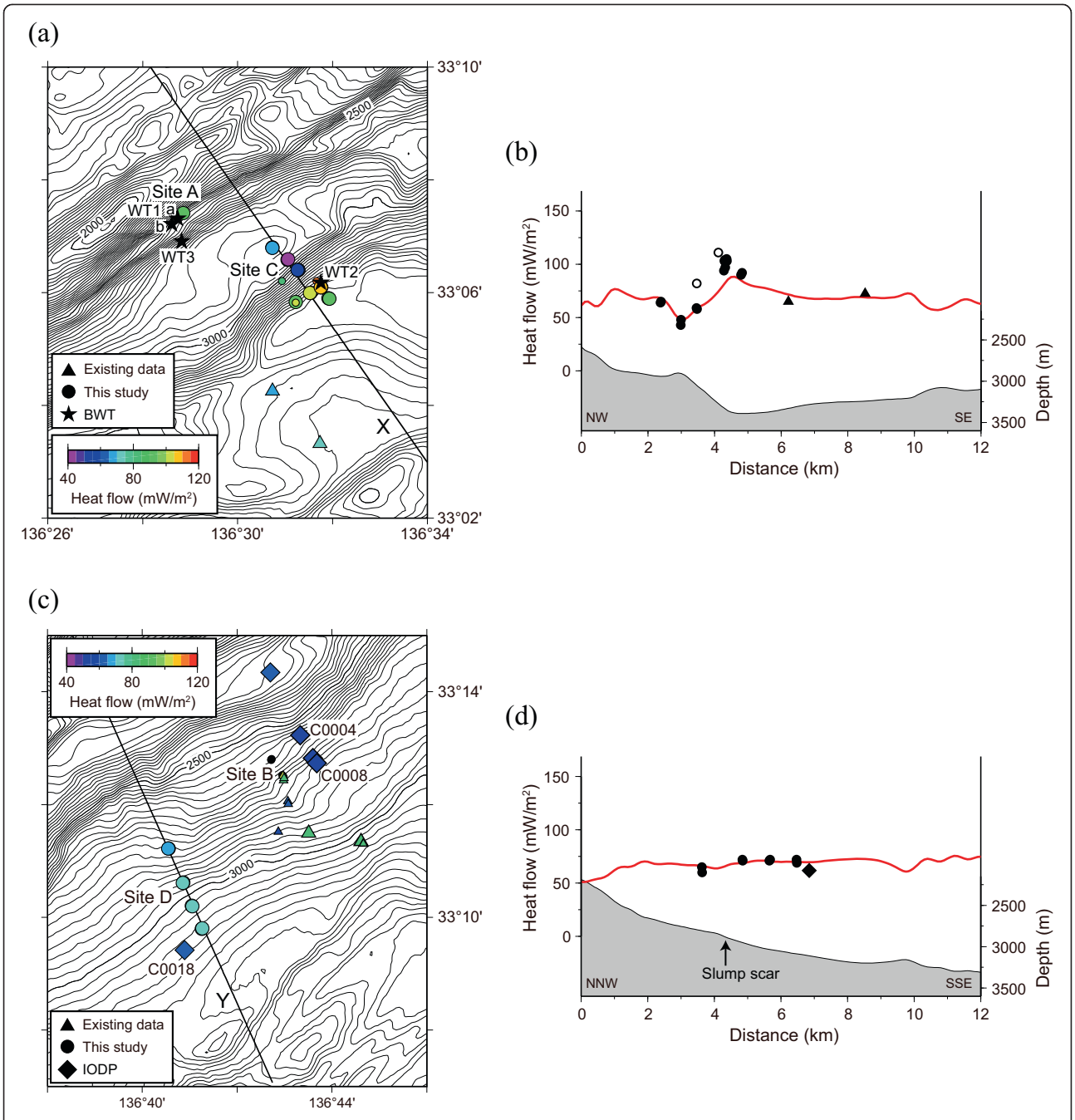

Figure 3 Heat flow data in detailed survey areas. (a) Heat flow data in area I (Figure 2) color-coded by heat flow value (triangles represent previous probe measurements; circles represent this study). Smaller symbols represent data of low quality. Stars are BWT monitoring stations. **(b)** Heat flow and bathymetry cross sections along line X in **(a)**. The red curve is the heat flow disturbed by the 2-D topographic effect for the background heat flow of 65 mW/m^2. Open circles are data of low quality. **(c)** Same as the data shown in **(a)** but for area II (Figure 2). Rhombuses are data from IODP holes. Black dots represent stations where nonlinear sediment temperature profiles were obtained (site B). **(d)** Same as the data shown in **(b)** but for line Y in **(c)**.

effect is generally within 10%, though it can reach 15% in extreme cases. We need to collect more long-term temperature records at depths around 3,000 m to determine the critical depth for the influence of BWT variation on heat flow measurements with surface probes.

Heat flow measurements in the high scatter zone

To study the relationship between the scattered heat flow and tectonic activity around the splay fault, heat flow measurements with ordinary surface probes were conducted during research cruises in 2010 and 2011, in

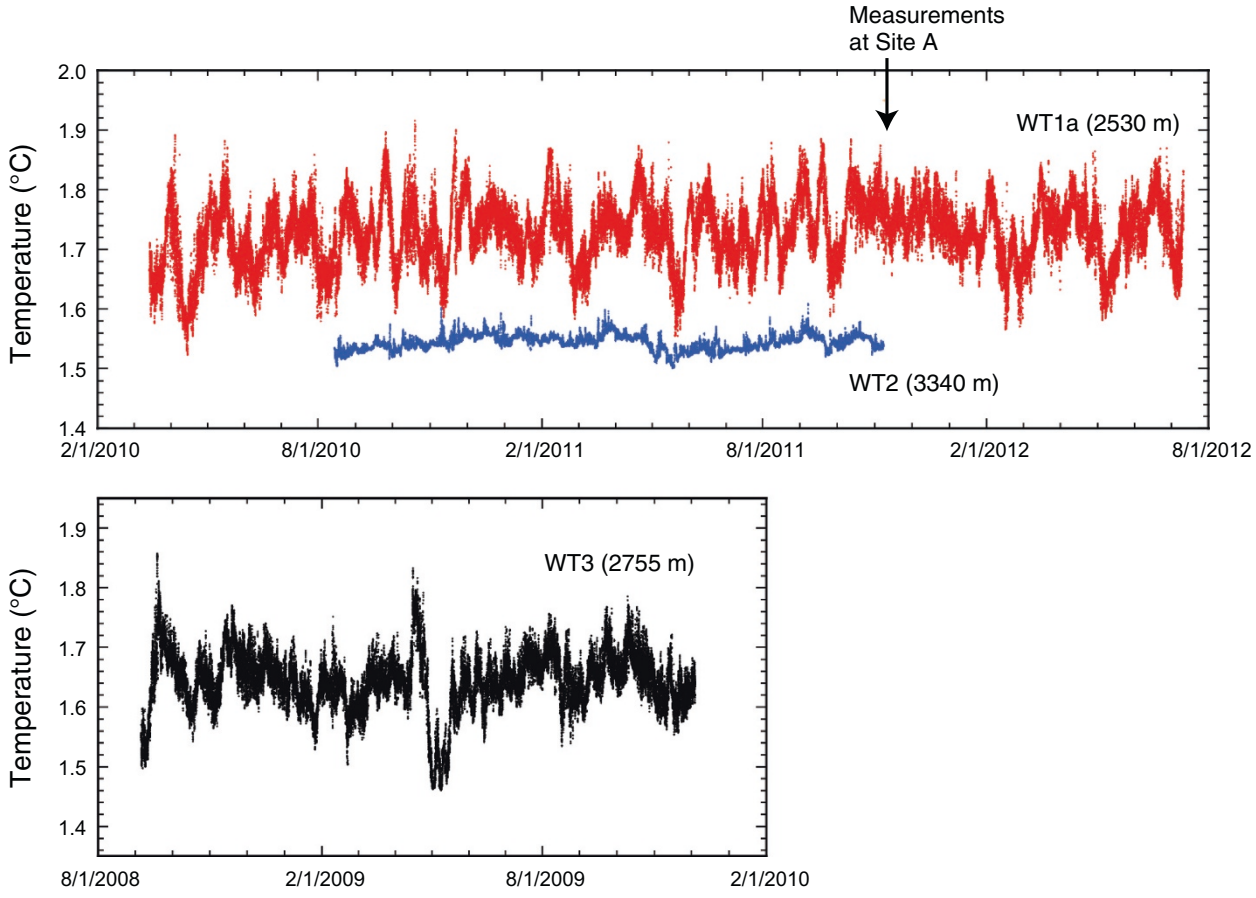

Figure 4 Time series of BWT at different water depths (WT1a, WT2, and WT3). Note that the observation period at WT3 does not overlap those at WT1a and WT2.

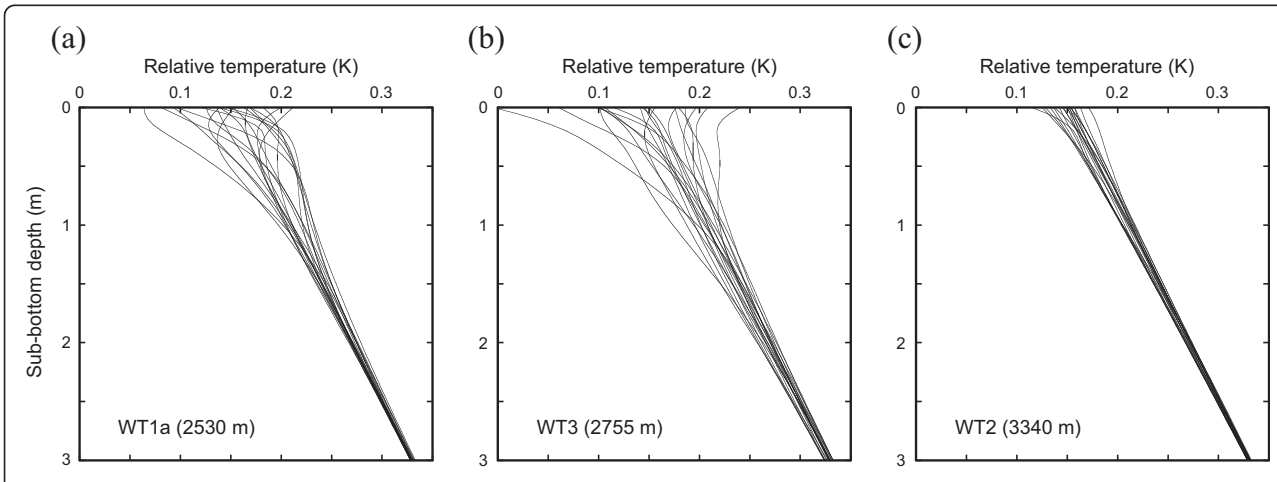

Figure 5 Disturbed sub-bottom temperature profiles calculated using the BWT records at WT1a (a), WT3 (b), and WT2 (c). The undisturbed temperature gradient and sediment thermal diffusivity are 60 mK/m and 3.0×10^{-7} m^2/s, respectively. Profiles at intervals of 15 days are shown for a certain 300-day period at each station.

parallel with BWT monitoring. We used 3-m long probes with seven temperature sensors, since longer probes often resulted in partial penetration in previous surveys. The measurements were made at the following four sites (Figures 2 and 3).

Site A: in the close vicinity of WT1a and cold seeps associated with the splay fault.

Site B: around the splay fault tip to the southwest of IODP Sites C0004 and C0008.

Site C: in the vicinity of a prominent fault scarp, along which biological communities were discovered.

Site D: in the middle part of the prism slope, close to IODP Site C0018.

The obtained data were classified into two groups: those of good quality where the probe penetrated over 1.5 m, and four or more sensors measured sediment temperature; and low quality where the probe penetration was less than 1.5 m or only three sensors were in the sediment. Different symbols (indicating size or shape) are used in Figures 2 and 3 to distinguish the two groups. We applied the same criteria to the existing data for plots in Figures 1, 2, and 3.

Correction for BWT variation

Site A is close to chemosynthetic biological communities that have been extensively investigated with geological, geochemical, and geophysical approaches (e.g., Ashi et al. 2002; Toki et al. 2004). BWT variations around these communities (water depth at around 2,550 m) are, however, too large for reliable heat flow measurements with ordinary surface probes, as evident from the BWT record at WT1a (Figure 5a). We therefore conducted measurements in the vicinity of BWT station WT1a during the monitoring period so that corrections for the influence of BWT variation can be made. Site A is located about 250 m northeast of WT1a (Figure 3a), and the water depth is 2,580 m, about the same as that at WT1a, 2,530 m. The short distance and small depth difference between the two sites allow us to use the BWT record at WT1a to correct the disturbed temperature profiles measured at site A.

The 3-m long probe fully penetrated three times 600 days after the start of BWT monitoring at WT1a (Figure 4). We calculated the disturbance in sediment temperature at the time of the probe measurement from the preceding BWT record. The sediment temperatures measured with the seven sensors were compared with the calculated disturbance added to various values of undisturbed temperature gradient (Figure 6). We can then determine the temperature gradient by choosing the value, which gives a good fit to the measured temperatures. In this fitting process, the probe penetration depth should be treated as an unknown parameter. The obtained temperature gradient varies with penetration from 84 to 97 mK/m, and the estimated error in the gradient is about 3 mK/m for each penetration. The sediment thermal diffusivity was assumed to be uniform, 3.0×10^{-7} m^2/s, but small variations in the diffusivity do not affect the results. With the average thermal conductivity of surface sediments on the prism slope in the off-Kumano area, 1.04 W/m/K (Hamamoto et al. 2011), heat flow at site A is calculated to be 85 to 105 mW/m^2.

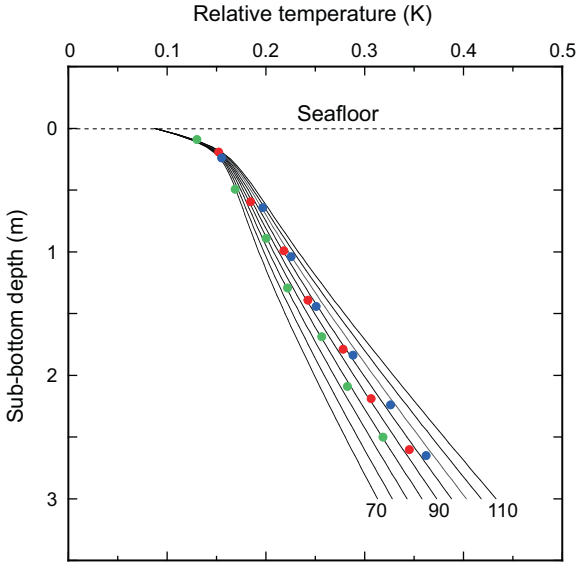

Figure 6 Sediment temperatures measured at site A fitted to temperature profiles calculated using the BWT record at WT1a. Red, green, and blue dots represent temperatures measured at the first, second, and third penetrations, respectively. The temperature profiles correspond to undisturbed gradients of 70 to 110 mK/m.

The above example demonstrates that a combination of long-term BWT monitoring and temperature profile measurement with a surface probe is a practical method of heat flow determination in areas with large amplitude BWT variations. The resolution of temperature gradient (heat flow) is higher with a deeper penetration depth and a larger number of sensors. Temperature profile measurements at different times during BWT monitoring will also reduce the error in heat flow determination.

The water depths of the measurement points at site B are 2,600 to 2,700 m, in the range for which we inferred that subsurface temperature is significantly disturbed by BWT variation ('Monitoring of bottom water temperature variation' section). The measured temperature profiles were actually curved and thus could not be used for heat flow determination.

Measurements around a fault scarp and a slump scar

We selected site C to investigate a large-scale heat flow distribution around a branch of the splay fault. At this site, the fault forms a nearly 500-m high scarp (Figure 3a), and the fault tip reaches the surface at the foot of the scarp. We conducted measurements along a line crossing the scarp (line X in Figure 3a) to examine the heat flow variation with distance from the fault. The water depths of the measurement points range from 2,910 to 3,365 m, and the influence of BWT variation is expected to be small on the seaward side of the scarp. The obtained temperature profiles were almost linear, giving no clear indication of the BWT variation effect.

Heat flow data at site C are plotted on the bathymetry profile along line X, together with nearby existing data (Figure 3b). Heat flow is apparently higher around the foot of the scarp than around the top of the scarp. It should be noted that refraction of heat flux due to the topographic effect also yields a similar pattern of surface heat flow variation. We calculated the topographic disturbance along line X, assuming two-dimensional bathymetry based on the formulation by Blackwell et al. (1980). The seafloor was treated as an isothermal boundary, since the spatial and temporal variations in BWT, less than 0.4 K (Figure 4), are much smaller than subsurface temperature variations due to topographic relief of the order of 100 m. The calculated surface heat flow (red curve in Figure 3b) is concordant with the observed heat flow, implying that the overall heat flow distribution across the scarp is attributable to the effect of bathymetric relief.

The highest values, about 100 mW/m^2, measured on the lower part of the scarp are even higher than those expected from the bathymetry. The locations of these high values were not precisely determined for the lack of information on the position of the heat flow probe relative to the ship. The water depths of the penetration points measured by the probe, however, evidently indicate that they are located on the lowest part of the scarp. Since biological activity related to cold seeps had been observed at about the same water depth, the local high heat flow probably arises from upward fluid flow along the fault.

The heat flow data at site C have another important implication. Except for the local high values discussed above, the heat flow distribution is well reproduced by the topographic disturbance with a background heat flow of 65 mW/m^2 (Figure 3b). Considering that the influence of BWT variation is minor seaward of the scarp, heat flow from depths at site C is inferred to be about 65 mW/m^2. The approximate range of heat flow values at site C, corrected for the topographic effect, is shown in Figure 1b, together with those for sites A and D (shaded red).

Site D is located on a gentle slope, and eight measurements were made at four points along line Y in Figure 3c. The water depths are from 2,790 to 3,075 m, in the range where the influence of BWT variation may not be negligible, though the obtained temperature profiles were linear. The measured heat flow is very uniform and shows no systematic variation along the line. Line Y crosses one of the slump scars of the submarine landslides pervasively distributed on the upper prism slope off Kumano (Kimura et al. 2011). Piston core samples taken on the down-dip side of the scar contained no mass transport deposits, which indicate that landslides corresponding to the scar did not occur recently (T. Kanamatsu, personal communication 2014). This is consistent with the observed uniform heat flow along the line.

The topographic effect at site D is small because of smooth bathymetry along line Y (Figure 3d). The measured heat flow values agree well with the calculated ones for a background heat flow of 65 mW/m^2. This value is consistent with the one measured in a borehole in the vicinity of line Y, IODP Site C0018, 62 mW/m^2 (Marcaillou et al. 2012) (Figure 3c,d), which cannot be affected by BWT variation. These results suggest that the heat flow from the depths at site D is about 65 mW/m^2, which is coincident with that at site C.

Discussion and conclusions

Long-term BWT records showed that the BWT variation is large enough to have a significant influence on heat flow measurements with surface probes to water depths of at least 2,755 m (WT3), while the influence is small at 3,340 m (WT2). Nonlinear sediment temperature profiles obtained at sites A and B with water depths from 2,575 to 2,740 m are thus interpreted as the effect of BWT variation. Linear temperature profiles and uniform heat flow observed at site D at water depths from 2,790 to 3,075 m suggest that the BWT effect was small at the

time of the measurements. However, this may not always be the case, because the BWT effect varies with time, even at a station that suffers large amplitude BWT variations, as demonstrated in Figure 5.

Based on the above discussion, we may suppose that the existing heat flow data measured at water depths less than 2,800 m could have been disturbed by BWT variation. Then, about half of the data in the high scatter zone, including the highest value, can be eliminated, which appreciably reduces the scatter. Variability of BSR-derived heat flow should provide information on the contribution of BWT variation to the scattered surface heat flow, because the temperatures at BSR depths (several hundred meters below the seafloor) are hardly affected by BWT variation. In our study area, however, BSRs are distributed seaward of the surface probe data (Kinoshita et al. 2011) and cannot be used for comparison. For further discussion, we obviously need long-term BWT records between 2,755 and 3,340 m.

At site C, heat flow corrected for the topographic effect is about 65 mW/m^2, except for local high values on the lowest part of the fault scarp. This value coincides with the uniform heat flow observed at site D and heat flow measured in a nearby borehole (IODP Site C00018). From these results, we infer that the heat flow from the deep, not affected by surface disturbances, is about 65 mW/m^2 around these sites located 20 to 25 km from the deformation front (Figure 1b). A value of 65 mW/m^2 at 20 to 25 km is consistent with the surface heat flow calculated with various subduction thermal models for the off-Kumano area (Harris et al. 2013).

Heat flow measured at site A, 85 to 105 mW/m^2, is appreciably higher than the regional heat flow estimated above, 65 mW/m^2 (Figure 1). The high anomaly becomes more marked if it is compared with about 50 mW/m^2 at IODP Sites C0004 and C008 (Harris et al. 2011) (Figure 2). Site A is located at a terrace on the middle part of a steep fault scarp (Figure 3a). The topographic effect on surface heat flow at this site is estimated to be relatively small, within 10 mW/m^2. The high heat flow cannot, therefore, be attributed to its bathymetric location.

Cold seeps accompanying biological communities were discovered at multiple locations along the terrace on which site A is located (e.g., Toki et al. 2004). Heat flow values had been obtained at some of the seep sites by analyzing long-term records of sediment temperature profiles (Goto et al. 2008). High conductive heat flow, over 100 mW/m^2, was measured at points several meters away from bacterial mats. Inside of bacterial mats, the temperature records indicate advective heat transport by upward fluid flow. These measurements were conducted with precise navigation and visual observation using submersibles and revealed local high heat flow at the scale of 10 m.

In contrast, high heat flow at site A and on the lowest part of the fault scarp at site C was obtained with ordinary heat flow probes lowered from a ship. The positions of measurement points were thus not well controlled with reference to bathymetric and geological features and/or biological activities. The results at sites A and C therefore show that high heat flow anomalies in a larger scale (of the order of 100 m) exist around the tips of the branches of the splay fault. This indicates that upward pore fluid flow may be occurring pervasively along the fault branches, yielding elevated heat flow zones along the fault tips. More precisely navigated measurements with an acoustic transponder system will allow us to map the extent of the high heat flow anomalies.

Competing interests
The authors declare that they have no competing interests.

Authors' contributions
MY conducted heat flow and water temperature measurements, analyzed the data, and drafted the manuscript. YK conducted heat flow and water temperature measurements, analyzed the data, and made model calculations. HH conducted temperature measurements and analyzed the data. All authors read and approved the final manuscript.

Acknowledgements
We are grateful to the officers, crews, and scientific parties of cruises KH-10-3 and KH-11-9 of the R/V Hakuho-maru for their assistance with the heat flow measurements. We also thank S. Goto for useful discussions and anonymous reviewers for valuable comments on the first version of the manuscript. This study was conducted as a part of the sub-project 'Recent activity of seismogenic faults' of the KANAME project (New perspective of great subduction-zone earthquakes from the super deep drilling) and supported by MEXT KAKENHI Grant Number 21107003.

Author details
[1]Earthquake Research Institute, University of Tokyo, 1-1-1 Yayoi, Bunkyo-ku Tokyo 113-0032, Japan. [2]Center for Environmental Science in Saitama, 914 Kami-tanadare, Kazo 347-0115, Japan.

Received: 6 March 2014 Accepted: 11 September 2014
Published: 2 October 2014

References
Ashi J, Tokuyama H, Ujiie Y, Taira A (1999) Heat flow estimation from gas hydrate BSRs in the Nankai Trough: implications for thermal structures of the Shikoku Basin. Eos Trans AGU 80(46):F929, Fall Meet Suppl, Abstract T12A–02

Ashi J, Kuramoto S, Morita S, Tsunogai U, Goto S, Kojima S, Okamoto T, Ishimura T, Ijiri A, Toki T, Kudo S, Asai S, Utsumi M (2002) Structure and cold seep of the Nankai accretionary prism off Kumano—outline of the off Kumano survey during YK01-04 Leg 2 Cruise. JAMSTEC J Deep Sea Res 20:1–8

Blackwell DD, Steele JL, Brott CA (1980) The terrain effect on terrestrial heat flow. J Geophy Res Solid Earth 85:4757–4772. doi:10.1029/JB085iB09p04757

Davis EE (1988) Oceanic heat-flow density. In: Haenel R, Rybach L, Stegena L (eds) Handbook of Terrestrial Heat-Flow Density Determination. Kluwer, Dordrecht, pp 223–260

Foucher JP, LePichon X, Lallemant S, Hobart MA, Henry P, Benedetti M, Westbrook GK, Langseth MG (1990) Heat flow, tectonics, and fluid circulation at the toe of the Barbados Ridge Accretionary Prism. J Geophys Res 95:8859–8867. doi:10.1029/JB095iB06p08859

Goto S, Hamamoto H, Yamano M, Kinoshita M, Ashi J (2008) Long-term temperature monitoring at the biological community site on the Nankai accretionary prism off Kii Peninsula. Eos Trans AGU 89(53):F2555, Fall Meet Suppl, Abstract T31A–1979

Hamamoto H, Yamano M, Goto S (2005) Heat flow measurement in shallow seas through long-term temperature monitoring. Geophys Res Lett 32(21), L21311. doi:10.1029/2005gl024138

Hamamoto H, Yamano M, Goto S, Kinoshita M, Fujino K, Wang K (2011) Heat flow distribution and thermal structure of the Nankai subduction zone off the Kii Peninsula. Geochem Geophys Geosyst 12:Q0AD20, doi:10.1029/2011gc003623

Harris RN, Schmidt-Schierhorn F, Spinelli G (2011) Heat flow along the NanTroSEIZE transect: results from IODP Expeditions 315 and 316 offshore the Kii Peninsula, Japan. Geochem Geophys Geosyst 12:Q0AD16, doi:10.1029/2011gc003593

Harris R, Yamano M, Kinoshita M, Spinelli G, Hamamoto H, Ashi J (2013) A synthesis of heat flow determinations and thermal modeling along the Nankai Trough, Japan. J Geophys Res Solid Earth 118:2687–2702. doi:10.1002/jgrb.50230

Henry P, Foucher J-P, Le Pichon X, Sibuet M, Kobayashi K, Tarits P, Chamot-Rooke N, Furuta T, Schultheiss P (1992) Interpretation of temperature measurements from the Kaiko–Nankai cruise: modeling of fluid flow in clam colonies. Earth Planet Sci Lett 109:355–371. doi:10.1016/S0025-3227(02)00262-1

Kawada Y, Toki T, Kinoshita M, Joshima M, Higa R, Kasaya T, Tsunogai U, Nishimura K, Kisimoto K (2014) Tracing geologically constrained fluid flow pathways using a combination of heat flow measurements, pore water chemistry, and acoustic imaging near the deformation front of the Nankai Trough off the Muroto Peninsula, Japan. Tectonophysics 618:121–137. doi:10.1016/j.tecto.2014.01.035

Kimura G, Moore GF, Strasser M, Screaton E, Curewitz D, Streiff C, Tobin H (2011) Spatial and temporal evolution of the megasplay fault in the Nankai Trough. Geochem Geophys Geosyst 12:Q0A008, doi:10.1029/2010gc003335

Kinoshita M, Yamano M (1995) Heat flow distribution in the Nankai Trough region. In: Tokuyama H, Shcheka S, Isezaki N et al (eds) Geology and Geophysics of the Philippine Sea. Terra Scientific Publishing Company (TERRAPUB), Tokyo, pp 77–86

Kinoshita M, Kanamatsu T, Kawamura K, Shibata T, Hamamoto H, Fujino K (2008) Heat flow distribution on the floor of Nankai Trough off Kumano and implications for the geothermal regime of subducting sediments. JAMSTEC Rep Res Dev 8:13–28. doi:10.5918/jamstecr.8.13

Kinoshita M, Moore GF, Kido YN (2011) Heat flow estimated from BSR and IODP borehole data: implication of recent uplift and erosion of the imbricate thrust zone in the Nankai Trough off Kumano. Geochem Geophys Geosyst 12:Q0AD18, doi:10.1029/2011gc003609

Marcaillou B, Henry P, Kinoshita M, Kanamatsu T, Screaton E, Daigle H, Harcouët-Menou V, Lee Y, Matsubayashi O, Kyaw Thu M, Kodaira S, Yamano M, Expedition IODP, 333 Scientific Party (2012) Seismogenic zone temperatures and heat-flow anomalies in the To-nankai margin segment based on temperature data from IODP expedition 333 and thermal model. Earth Planet Sci Lett 349–350:171–185. doi:10.1016/j.epsl.2012.06.048

Martin V, Henry P, Nouzé H, Noble M, Ashi J, Pascal G (2004) Erosion and sedimentation as processes controlling the BSR-derived heat flow on the Eastern Nankai margin. Earth Planet Sci Lett 222:131–144. doi:10.1016/j.epsl.2004.02.020

Moore GF, Park J-O, Bangs NL, Gulick SP, Tobin HJ, Nakamura Y, Sato S, Tsuji T, Yoro T, Tanaka H, Uraki S, Kido Y, Sanada Y, Kuramoto S, Taira A (2009) Structural and seismic stratigraphic framework of the NanTroSEIZE Stage 1 transect. Proc Integr Ocean Drill Program, 314/315/316. doi:10.2204/iodp.proc.314315316.102.2009

Osada Y, Kido M, Fujimoto H (2010) Observation of seafloor crustal movement on Kumano-nada prism slope. Paper presented at the Seismological Society of Japan, Fall Meeting, Hiroshima, 27–29 October 2010, Abstract P2–48

Park J, Kodaira S (2012) Seismic reflection and bathymetric evidences for the Nankai earthquake rupture across a stable segment-boundary. Earth Planets Space 64:299–303. doi:10.5047/eps.2011.10.006

Park J-O, Tsuru T, Kodaira S, Cummins PR, Kaneda Y (2002) Splay fault branching along the Nankai subduction zone. Science 297:1157–1160. doi:10.1126/science.1074111

Spinelli GA, Harris RN (2011) Thermal effects of hydrothermal circulation and seamount subduction: temperatures in the Nankai Trough Seismogenic Zone Experiment transect, Japan. Geochem Geophys Geosyst 12:Q0AD21, doi:10.1029/2011gc003727

Strasser M, Moore GF, Kimura G, Kopf AJ, Underwood MB, Guo J, Screaton EJ (2011) Slumping and mass transport deposition in the Nankai fore arc: evidence from IODP drilling and 3-D reflection seismic data. Geochem Geophys Geosyst 12:Q0AD13, doi:10.1029/2010gc003431

Tobin HJ, Kinoshita M (2006) NanTroSEIZE: the IODP Nankai Trough Seismogenic zone experiment. Sci Drill 2:23–27. doi:10.2204/iodp.sd.2.06.2006

Toki T, Tsunogai U, Gamo T, Kuramoto S, Ashi J (2004) Detection of low-chloride fluids beneath a cold seep field on the Nankai accretionary wedge off Kumano, south of Japan. Earth Planet Sci Lett 228:37–47. doi:10.1016/j.epsl.2004.09.007

Yamano M, Kinoshita M, Goto S, Matsubayashi O (2003) Extremely high heat flow anomaly in the middle part of the Nankai Trough. Phys Chem Earth Parts A/B/C 28:487–497. doi:10.1016/S1474-7065(03)00068-8

Zwart G, Moore JC, Cochrane GR (1996) Variations in temperature gradients identify active faults in the Oregon accretionary prism. Earth Planet Sci Lett 139:485–495. doi:10.1016/0012-821X(95)00244-7

doi:10.1186/1880-5981-66-126
Cite this article as: Yamano *et al.*: **Heat flow survey in the vicinity of the branches of the megasplay fault in the Nankai accretionary prism.** *Earth, Planets and Space* 2014 **66**:126.